Self-aligning atomic strings in surface-supported biomolecular gratings

Agustin Schiffrin,[1,*] Joachim Reichert,[2,3] Willi Auwärter,[3] Gesine Jahnz,[2] Yan Pennec,[2] Alexander Weber-Bargioni,[2] Valeri S. Stepanyuk,[4] Larissa Niebergall,[4] Patrick Bruno,[4,5] and Johannes V. Barth[1,2,3,†]

[1]*Department of Chemistry, UBC Vancouver, British Columbia, Canada V6T 1Z4*

[2]*Department of Physics and Astronomy, UBC Vancouver, British Columbia, Canada V6T 1Z4*

[3]*Physik Department E20, TU München, James-Franck Strasse, D-85748 Garching, Germany*

[4]*Max-Planck-Institut für Mikrostrukturphysik, Weinberg 2, 06120 Halle, Germany*

[5]*European Synchrotron Radiation Facility, BP 220F, 38043 Grenoble Cedex, France*

(Received 27 March 2008; revised manuscript received 12 June 2008; published 15 July 2008)

We demonstrate the one-dimensional ordering of Co and Fe atoms employing supramolecular templates. Our low-temperature scanning tunneling microscopy observations reveal how individual adatoms spontaneously align with a preferred ~25 Å next-neighbor spacing in self-assembled methionine nanogratings on Ag(111). For Co strings the pertaining equilibrium statistics and dynamics were monitored to assess the underlying long-range interactions with their anisotropic energy landscape. The effect of the surface-state electron quantum confinement on the atomic self-alignment is revealed by tunneling spectroscopy mapping and *ab initio* calculations.

DOI: 10.1103/PhysRevB.78.035424 PACS number(s): 81.16.Dn, 81.16.Fg, 68.37.Ef, 07.79.Cz

I. INTRODUCTION

The positioning of single adsorbed species on surfaces or in nanostructured environments is an ultimate precision method for the exploration of quantum physics in reduced dimensions. Notably the manipulation of individual adsorbed atoms and self-assembly techniques have been used to engineer quantum systems, whereby linear arrangements revealed unique magnetic and electronic properties. Thus quantum corrals and mirages have been realized with the positioning of single atoms by the tip of a scanning tunneling microscope (STM).[1,2] Artificial atomic chains showed the development of one-dimensional (1D) band structure[3,4] or even ferromagnetic order.[5] Complementary to atomic manipulation and self-organized growth strategies, supramolecular self-assembly on solid surfaces provides highly organized systems with molecular-level feature control.[6–11] Using appropriate protocols it is possible to achieve low-dimensional nanostructures such as hydrogen-bonded supramolecular gratings[8,9] or two-dimensional (2D) metal-organic coordination networks,[12,13] whereby nanoporous systems provide specific templates to accommodate and organize functional guest molecules.[7,14]

When close-packed noble-metal surfaces are employed as construction platforms, their electronic configuration influences sensitively the structural characteristics and physical properties. Notably, the influence of the surface-state band on atomic self-ordering on metal surfaces has been extensively studied in the past, both experimentally[15–19] and theoretically,[20–25] including the recent model-based hypothesis of adatom organization in quantum corrals.[24] Adsorbed molecules and atoms, and other defects such as step edges, perturb the surface electronic states by scattering and confining the substrate electrons,[1,26,27] which can even lead to partial or total depopulation of the band.[27,28] Tuning the substrate surface-state band by electronically confining nanotemplates of well-defined morphology offers a supplementary genuine control parameter to develop self-assembly methodologies.

Here we present a low-temperature STM and scanning tunneling spectroscopy (STS) study of the self-alignment of Fe and Co adatoms in regular methionine biomolecular nanogratings on Ag(111). The transition-metal species, which are immobile in the trenches at low temperature, are found to spontaneously order into 1D chains once they are annealed to 18 K. Within these 1D nanostructures, the metallic atoms are regularly distributed following a nonrandom trend: we find for the Fe chains a most probable nearest-neighbor distance of 23 Å, whereas for Co it is of 25 Å. These values reveal a long-range interaction which is mediated by the electronic structure of the underlying Ag(111) substrate, similarly to findings for 2D hexagonal atomic lattices.[16–18] For the case of the Co, the dynamics of the ordering process could be monitored: first adatom diffusion can be observed at 15 K and they align into a 1D chain at 18 K, whereby their motions obey an Arrhenius law with a decreased mobility in comparison to isolated adatoms on the bare Ag(111) substrate. This restrained atomic motion appears in our measurements of the hopping rates. The one-dimensional self-ordering is associated with long-range row-adatom and adatom-adatom interactions mediated by the Ag(111) surface-state electrons. To test this hypothesis, we model the respective interaction potential mediated by the substrate electronic configuration using the Korringa-Kohn-Rostocker (KKR) Green's function method[20–24,29] providing a very satisfactory agreement with the experimental data.

II. EXPERIMENT

The experiments for this study were carried out in a custom-designed ultrahigh-vacuum (UHV) chamber operating at a base pressure of $\sim 2\times 10^{-10}$ mbar and equipped with a commercial He bath-cryostat low-temperature STM (Ref. 30) based on a design described in Ref. 31. The sample preparation was performed *in situ*: the chemomechanically polished Ag(111) monocrystalline substrate (lattice constant of 2.89 Å at 300 K) was cleaned by repeated Ar^+ sputtering

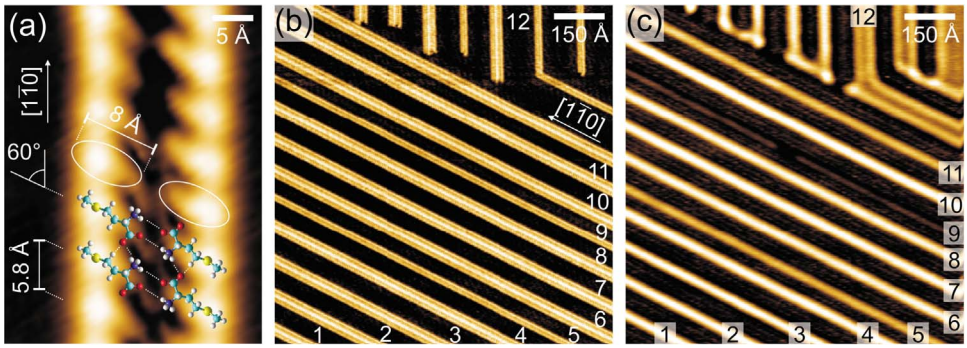

FIG. 1. (Color online) STM and STS data of the methionine biomolecular nanogratings on Ag(111) and the resulting quantum well states. (a) STM topographical data of the biomolecular arrangement within a *L*-methionine double row (I=0.9 nA, U=−80 mV). Color code for the molecular model: cyan (C), blue (N), red (O), yellow (S), and white (H). (b) STM image of a methionine nanograting with bare Ag(111) trenches of average width of ~45 Å, i.e., electronic confinement length of ~65 Å. The bare Ag(111) trenches in between the biomolecular rows are numbered from 1 to 12 (I=0.1 nA, U=−34 mV, Θ_{mol}=0.43 ML). (c) dI/dV map of the methionine/Ag(111) system in (b): the quasi-two-dimensional surface-state electron gas is subject to one-dimensional confinement in undecorated Ag(111) trenches (I=0.1 nA, U=−34 mV).

cycles at an energy of 0.8 keV, followed by annealing at a temperature of 770 K for ~10 min. The enantiopure methionine amino acid molecules (purity >99.5%, Sigma-Aldrich) were vapor deposited onto the Ag(111) substrate from a crucible heated at a temperature of 370 K, with the substrate held at 320 K. After preparation, the sample is cooled down to $T<10$ K for Fe or Co adatom deposition and STM and STS measurements. The Fe and Co adatoms are evaporated *in situ* onto the sample from a properly degassed pure filament of Fe and Co wound around a W wire. The STM and STS data are obtained with an electrochemically etched W tip, with the bias voltage applied to the sample, and in a temperature range from 8 to 18 K, the sample temperature being regulated with a Zener diode and measured with a Si diode. STM topographical images correspond to constant-current data. The dI/dV maps are obtained with a lock-in technique, with measurements typically performed with a 5 mV rms and ~3 kHz modulation. STM and STS data were treated with the WSXM software package.[32]

III. RESULTS AND DISCUSSION

The methionine amino acid deposited onto a Ag(111) substrate at ~320 K self-assembles into regular 1D nanogratings which follow the ⟨110⟩ crystalline orientations of the underlying substrate[9] and thus bear similarities with the supramolecular arrangement of other functional molecular species on the same surface.[8,33] Figure 1(a) depicts the amino acid arrangement within a double *L*-methionine chain. These 1D biomolecular rows spread in unidirectional mesoscopic domains reaching several μm^2. For molecular coverages between 0.1 and 0.6 ML, the interchain separation can be tuned between widths of 20 and 200 Å. The amino acid species are thereby in their zwitterionic chemical state, and the supramolecular 1D nanostructures consist in molecules dimerizing and bonding adjacently through hydrogen bonds involving the carboxylate and ammonium groups. Double or quadruple molecular rows coexist in the shown assembly, quadruple rows corresponding to two merged double chains. The difference between the *L*-methionine and *D*-methionine homochiral self-assemblies is exclusively in the intrachain molecular arrangement; the *D* molecular dimer is oriented at a −60° angle with respect to the 1D chain growth orientation, whereas the *L*-dimer forms an angle of +60°. Otherwise, the morphologies of the *L* and *D* self-assemblies are identical, as well as their influence on the electronic properties of the Ag(111) surface. Consequently we do not specify the chirality characteristics of the systems investigated in the following. In this study, only results related to homochiral preparations are presented.

Figure 1(b) depicts a topographical constant-current STM image of a self-assembled regular methionine nanograting. Thinner and wider stripes correspond, respectively, to double and quadruple biomolecular chains.[9] The black colored stripes are bare Ag(111) trenches (numbered from 1 to 12). Here, the average width of the trenches is 45 Å, which corresponds to an electronic confinement length of ~65 Å.[27] The amino acid self-assembly perturbs the electronic properties of the underlying Ag(111) substrate by locally quenching the surface state. The surface-state electrons thus become confined into the bare patches of silver; the biomolecular trenches act as nanoscale quantum resonators.[27] The definition of the electronic confinement length is extracted from a Fabry-Pérot model description. The local density of states of the system is visualized by the STS dI/dV map in Fig. 1(c) obtained at −34 mV; in the trenches we observe the electronic resonant modes caused by the electronic surface-state confinement, whereas this surface state is clearly quenched beneath the biomolecular rows. The confined surface-state band is shifted following a quadratic law with respect to the confinement length, analogously to the quantum particle-in-box system. In trench 9, for example, the electronic state is depopulated: the trench being too narrow, the surface-state onset is above the energy of −34 meV corresponding to this dI/dV map. On the other hand, we observe in the wider trench number 12 two maxima for the surface electronic density, corresponding to the second resonant mode. In general, the STS data reveal the remarkable homogeneity of the surface density of states within the individual trenches.

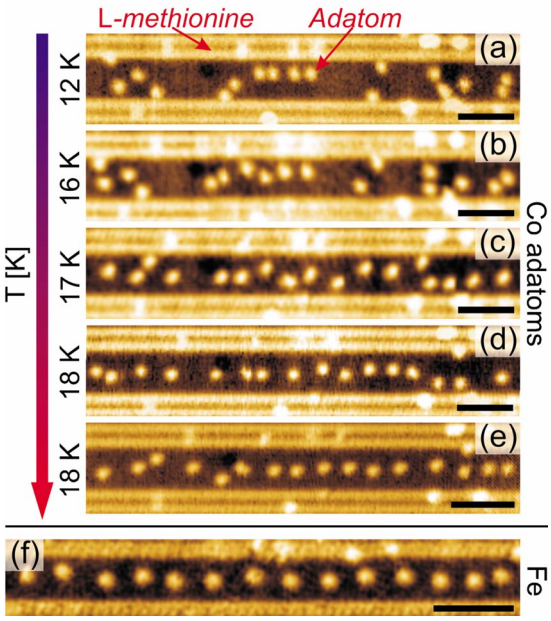

FIG. 2. (Color online) Adatom 1D self-alignment in between methionine biomolecular chains. [(a)–(e)] Randomly distributed Co adatoms at 12 K in the bare Ag(111) trenches self-align into regular chains after annealing to 18 K. The bare substrate trench is 35 Å wide, i.e., confinement length of ~55 Å. (f) Fe adatom row in a biomolecular nanograting with interchain distance of 25 Å, i.e., confinement length of ~45 Å. Image acquired at 12 K after annealing to 18 K (I=0.06 nA, U=−1770 mV). Scale bars: 50 Å.

After characterizing the molecular assembly, Fe or Co adatoms are deposited onto the methionine nanogratings on Ag(111) *in situ*, with the system held initially at 8 K. The adatom coverage Θ_{adatom} of both Co and Fe is typically chosen to be approximately 5×10^{-3} ML. First, we focus on a data set where the Co metal atoms were evaporated onto a methionine/Ag(111) preparation with a molecular coverage Θ_{mol} of ~0.43 ML, corresponding to an average biomolecular trench width of 35 Å with standard deviation of 2.9 Å. Herewith we illustrate the dynamics and self-alignment process of the metal atoms in the bare Ag(111) trenches in between the biomolecular nanogratings. Figure 2(a) shows a STM constant-current topographic image at 12 K of a 35 Å wide trench with Co adatoms on the Ag(111) patch. At this temperature, both Co and Fe single adatoms are frozen: they start to diffuse at a temperature of 15 K. During surface atomic diffusion, the experimental observation reveals hopping lengths of single Ag(111) lattice units. This demonstrates that the adatoms prefer specific adsorption sites with respect to the underlying substrate, which is in agreement with previous theoretical studies of other adatom/substrate systems.[34] When annealed at 18 K, the adatoms diffuse and self-arrange into 1D ordered chains in the middle of the trench, without forming any dimers or clusters.

Figures 2(a)–2(e) illustrate this self-ordering process of originally randomly distributed Co adatoms into regularly ordered 1D chains (the single protrusions at the methionine rows are captured Co atoms that serve simultanesouly as markers). The positioning of the atoms in the center of the trench and the regular spacing between the species reveal a mesoscale interaction with the biomolecular rows and in between the adatoms, respectively.

For comparison, the Fe alignment in Fig. 2(f) was obtained with a preparation with Θ_{mol} equals ~0.60 ML, giving substrate trenches with an average width of 25.5 Å and standard deviation of 5.0 Å. It reveals a regularly ordered Fe chain at 12 K after being annealed at 18 K: the initially frozen and disordered system diffuses at 18 K and organizes in a dynamic equilibrium dictated by Boltzmann statistics. For the case of Co adatoms, a corresponding movie is supplied as supplementary information.[35] Upon cooling, the single atomic species are trapped in the local minima of the 2D energy landscape imposed by the supporting substrate atomic lattice and the nanoscale local environment. The entropic pressure against which the self-aligning process competes has to become compensated by a gain in energy resulting from the interaction between the components of the system, i.e., the biomolecular assemblies and the metal adatoms.

The dynamics of the Co self-alignment in between methionine chains was followed at the single atom level and compared with the diffusion of isolated Co on a bare Ag(111) surface. For this purpose, we took into account the diffusion of ~200 cobalt adatoms in biomolecular trenches of 25–35 Å width. Their hopping rate was determined from STM data for temperatures between 15 and 18 K. A possible interference of the tunneling parameters was carefully considered, the outcome being that the experimental method does not perturb the intrinsic dynamics of the system. The measurements corresponding to the adatoms in between the biomolecular trenches were carried out with the tunneling parameters I_t=0.06 nA and U_{bias}=−400 mV, whereas for the bare Ag(111) the parameters I_t=0.1 nA and U_{bias}=−80 mV were taken. For isolated atoms and specific site adsorption (as observed experimentally), the adatom hopping rate Γ at a temperature T is given by

$$\Gamma(T) = -\frac{1}{\Delta t}\ln[P(\Delta t)]. \tag{1}$$

Here $P(\Delta t)$ is the probability that an adatom remains immobile after a delay time Δt.[36] $P(\Delta t)$ was evaluated experimentally by continuous sequences of STM images for the adatoms in between methionine trenches at the temperatures of 15 and 16 K, where single hopping events could be tracked from image to image. For the temperatures of 17.2 and 18 K, the imaging rate of our setup could not follow single events and the more general definition of Γ for an isolated adsorbate had to be considered,

$$\langle\|\Delta\vec{r}(\Delta t)\|^2\rangle = \Gamma\langle\lambda\rangle^2\Delta t, \tag{2}$$

with $\langle\lambda\rangle$ being the average hopping length and $\langle\|\Delta\vec{r}(\Delta t)\|^2\rangle$ the average square displacement of an adatom after time Δt. Assuming single hopping events, $\langle\lambda\rangle$ is equal to the atomic lattice constant, and Γ can be evaluated by measuring $\langle\|\Delta\vec{r}(\Delta t)\|^2\rangle$ through STM image sequences. This method is also used to determine Γ on the bare Ag(111) substrate. The use of this definition for Γ implicitly includes the hypothesis that the atomic mobility in the trenches follows an unre-

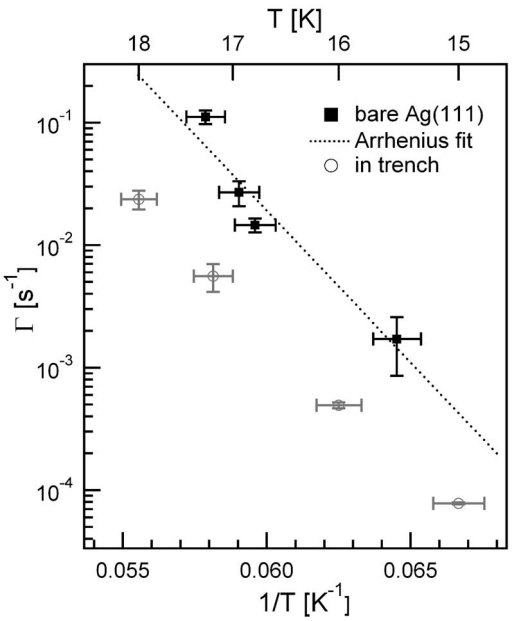

FIG. 3. Temperature dependence of Co adatom hopping rates. Compared to isolated atoms on bare Ag(111) (square black symbols), the mobility of Co confined in between methionine biomolecular trenches of 25–35 Å widths (circular gray symbols) is markedly reduced. Arrhenius fit parameters for the bare substrate case: $\Gamma_0 = 1.4 \times 10^{13\pm3}$ s^{-1}; $E_m = 49 \pm 9$ meV.

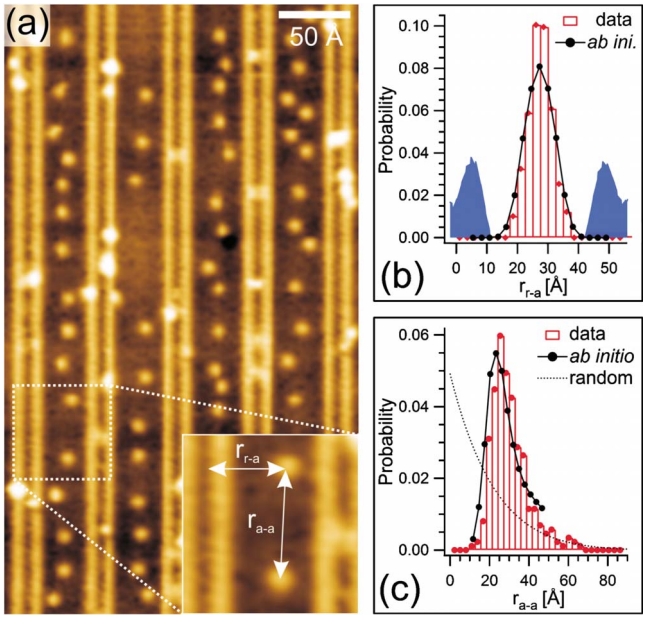

FIG. 4. (Color online) Statistics of adatom-chain and nearest-neighbor adatom-adatom distances in 35 Å wide methionine trenches. (a) STM topographical image of Co adatoms in between biomolecular trenches separated of 35 Å (confinement length of ~55 Å) at 18 K; r_{r-a} represents the adatom distance to the center of the amino acid row and r_{a-a} is the adatom-adatom nearest-neighbor distance (I=0.06 nA, U=−400 mV). (b) Experimental probability density of adatom-row distances r_{r-a} (in red). The Boltzmann theoretical probability density (in solid black) given by *ab initio* calculations matches the experimental data. The blue curve represents the height profile of the methionine rows. (c) Experimental probability density of adatom-adatom nearest-neighbor distances r_{a-a} (in red). The distribution indicates a nonrandom positioning of the adatoms in the trenches and can be fitted with a Boltzmann probability density derived with the results from *ab initio* calculations (black dots).

stricted random walk. This can seem abusive, but the approach is on the one hand necessary in order to compare the confined and free cases. On the other hand, care was taken to select data sets of adatoms near the center with displacements much smaller than the width of the silver trench. Because the energy landscape is rather flat there, a quantitative measure of the mobility is obtained (*vide infra*).

The experimental values of Γ in relation to T are plotted in Fig. 3. The motion of Co on the bare substrate is described by transition state theory (TST),[36] which states that the adsorbate diffusion is mediated by the substrate heat bath and that Γ follows an Arrhenius behavior: $\Gamma(T) = \Gamma_0 \exp(-E_m/k_B T)$, where E_m is the migration barrier and Γ_0 the prefactor. The experimental data yield for the bare case the values of $\Gamma_0 = 1.4 \times 10^{13\pm3}$ s^{-1} and $E_m = 49 \pm 9$ meV, which finding is in agreement with an earlier low-temperature STM analysis.[37] It is important to note that $k_B T \ll E_m$ in our temperature range, which is a necessary condition to model the adsorbate diffusion behavior with TST. In the considered temperature range, the hopping rates of the Co adatoms in the biomolecular trenches are decreased by about an order of magnitude with respect to those of isolated atomic species on the bare Ag(111) surface. This loss of mobility is a consequence of the atomic confinement within the biomolecular nanograting. A similar trend was encountered at appreciable coverages of Co adatoms on bare Ag(111), where long-range interactions between adatoms become operative.[38] If we assume that the mobility reduction leaves the prefactor unaffected (for related analysis, cf. Refs. 36 and 39), the corresponding increase in the migration energy barrier between adjacent sites with the adatoms residing close to equilibrium positions is estimated to approximately 5 meV.

The Co atomic self-alignment is quantitatively summarized in Fig. 4. Here, we tracked the movement of 11 Co adatoms at 18 K in a 35 Å wide trench (i.e., with an electronic confinement length of ~55 Å) within a sequence of 30 STM images and during a total acquisition time of ~10 000 s. The experimental data allowed us to evaluate the probability densities $p(r_{r-a})$ and $p(r_{a-a})$ of finding, respectively, an adatom within the distance interval $[r_{r-a}, r_{r-a}+dr_{r-a}]$ from the center of a methionine double row [Fig. 4(b)] and of finding a nearest neighbor within the distance interval $[r_{a-a}, r_{a-a}+dr_{a-a}]$ [Fig. 4(c)]. In a random configuration, the probability density of finding an adatom in a trench of width w at a distance r_{r-a} is equiprobable and is given by $1/w$. Figure 4(b) depicts the nonrandomness of the adatom distribution and of the 1D self-alignment: the adatoms strongly prefer the center of the trench and strictly avoid the molecular boundaries. This provides direct evidence of a repulsive interaction between adatoms and molecular walls.

Now, considering the adatom distribution in the direction along the rows, the random probability of finding a nearest-neighbor adatom at a distance r_{a-a} is given by

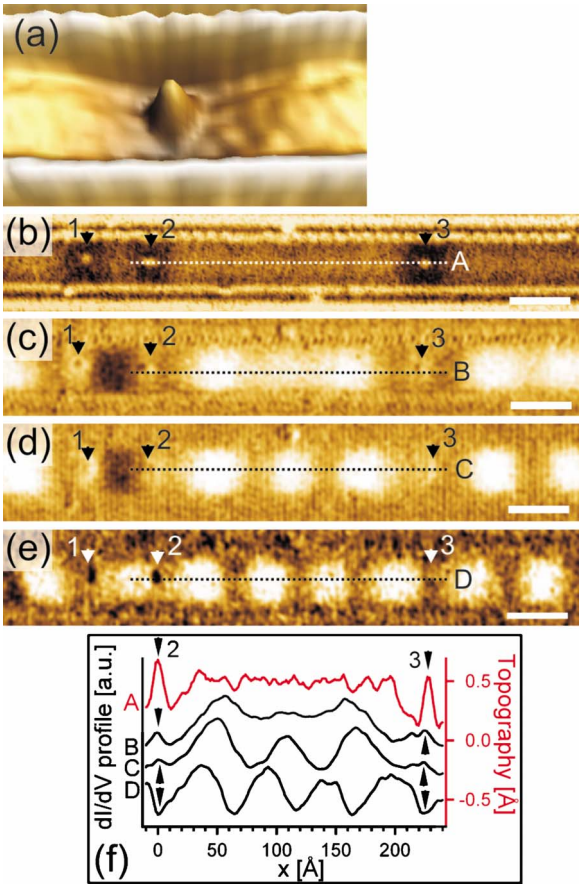

FIG. 5. (Color online) Confinement of surface electrons in methionine supramolecular nanostructures with Co adatoms: mediation of the repulsive interaction. (a) 3D representation of a single Co adatom on Ag(111) in between two methionine chains (I=0.1 nA, U=−20 mV). (b) STM topographical image of three Co adatoms in between methionine rows separated by 35 Å (I=0.06 nA, U=−80 mV). [(c)–(e)] dI/dV maps of the same location at U=−59 mV, U=−39 mV, and U=−9 mV, respectively (I =0.06 nA). Data acquired at 12 K, after annealing the sample to 16 K. Scale bars: 50 Å. (f) Intensity profiles of the constant-current STM topographic data (red) and of the STS first derivative maps along lines A–D. Different resonant modes appear at the selected bias voltages.

$$p_{\mathrm{ran}}^{1\mathrm{D}}(r_{a-a}) = \frac{2n}{L}\left(1 - \frac{2r_{a-a}}{L}\right)^{n-1}. \quad (3)$$

The first term represents the probability of finding an adatom in the distance interval $[r_{a-a}, r_{a-a}+dr_{a-a}]$, the second term the probability of not finding an adatom at a distance smaller than r_{a-a}, n the total number of adatoms, and L the trench length. The experimental probability density in Fig. 4(c) is a direct indication of the nonrandom 1D adatom distribution along the chains. Here, the most probable nearest-neighbor distance is 25.4 Å. A similar statistical study was performed for the Fe case, given a most probable nearest-neighbor distance of 23 Å.

The principal suspect to mediate the interaction enabling this self-ordering process is the electronic surface-state band

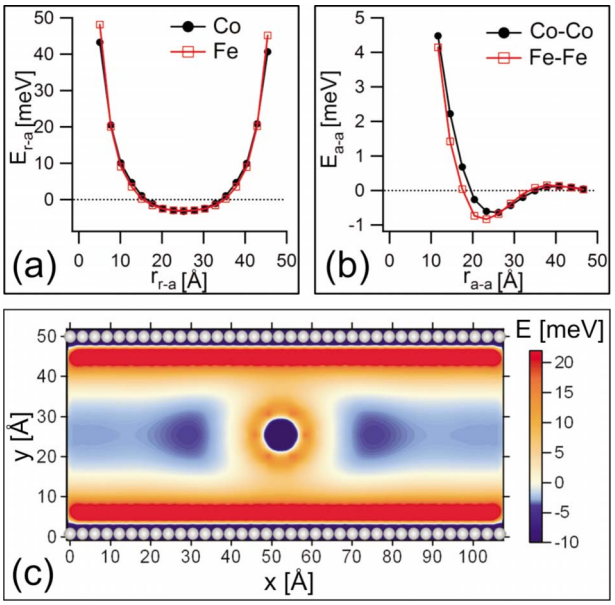

FIG. 6. (Color online) KKR Green's function calculations of the interaction energy between Fe and Co adatoms and a quantum resonator with 50 Å confinement length. (a) Plot of the interaction energy between adatom and resonator with respect to the row-adatom distance r_{r-a}. (b) Adatom-adatom interaction potential along the symmetry axis of a resonator revealing preferential spacings of ~26 Å for Co and ~23 Å for Fe, respectively. (c) 2D total interaction energy map for a system with one Co adatom positioned in the middle of the quantum resonator.

of the Ag(111) substrate, as previously demonstrated for atomic superlattices.[15–18,29] Figure 5 illustrates a low-density Co deposition onto the methionine/Ag(111) system, where three Co adatoms (labeled 1–3) are positioned in a 35 Å wide trench [Fig. 5(b)]. The STS dI/dV landscapes in Figs. 5(c)–5(e) are a direct measurement of the local density of states and show how the interchain adatoms scatter and confine the Ag(111) surface electrons in the trench; Co atoms 2 and 3 represent electronic scattering potentials and define boxlike border conditions for the surface electron eigenstates, which implies constructive electronic interferences (and thus electronic resonant states) only for specific energies. For instance, the spectroscopic maps of Figs. 5(c)–5(e), with bias voltages of −59, −39, and −9 mV, respectively, visualize the electron density of states close to the resonant modes of the surface electrons in the quantum well defined by the Co adatoms and the confining methionine chains. Figure 5(f) plots the apparent topographic (A) and spectroscopic profiles (B–D) along the trench and emphasizes the different surface electron modes.

To probe the hypothesis according to which the self-alignment is driven by the substrate electronic configuration, the row-adatom and adatom-adatom interaction energies were assessed theoretically using the KKR Green's function formalism.[15,21,23,24,29] The results are summarized in Fig. 6. The calculations are performed for both Co and Fe adatoms, and the system is modeled by positioning a metal adatom in the middle of a Ag(111) trench with a confinement length of 50 Å (simulating a biomolecular trench of 30 Å width). Be-

cause the methionine chains and the Ag(111) step edges have similar electronic scattering properties;[26,27] the biomolecular rows are actually modeled by two Ag step edges. Figure 6(a) represents the surface electron mediated interaction energy between the adatom and the rows. The results for Fe and Co are identical, and the energy minimum at the center of the trench steers the adatom 1D self-ordering. The theoretical adatom-adatom interaction in the chain direction which is mediated by the substrate is similar to that of adatom pairs on a pure Ag(111) surface. This interaction potential is plotted in Fig. 6(b). Finally, Fig. 6(c) represents the 2D energy landscape showing both the adatom-row and adatom-adatom interactions. The interatomic interaction is similar for Fe and Co, with an energy minimum positioned at a nearest-neighbor distance slightly smaller for Fe. The ~1 Å difference results from the different electron-scattering properties of the respective adatoms.

The theoretical results were compared with the experimental data by defining theoretical probability densities for $p(r_{r-a})$ and $p(r_{a-a})$ in the case of the Co adatoms, which are expressed assuming a Boltzmann equilibrium distribution as follows:

$$p(r_{r-a}) = \frac{1}{Z}\exp\left(\frac{-E_{r-a}(r_{r-a})}{k_B T}\right) \tag{4}$$

and

$$p(r_{a-a}) = \frac{1}{Z}p_{\mathrm{ran}}^{1\mathrm{D}}(r_{a-a})\exp\left(\frac{-E_{a-a}(r_{a-a})}{k_B T}\right), \tag{5}$$

with $p_{\mathrm{ran}}^{1\mathrm{D}}(r_{a-a})$ being the random 1D distribution defined above and Z the partition function guaranteeing a properly normalized distribution. These theoretical expressions are plotted in Figs. 4(b) and 4(c), where they are compared with the experimental statistics taken at 18 K. The confinement length taken in the theoretical approach being 50 Å and the one in the experiments of 55 Å, the abscissa of the theoretical distribution was rescaled by a factor of 1.1 for the $p(r_{r-a})$ case. The agreement between theory and experiment is remarkable, for both the cases of $p(r_{r-a})$ and $p(r_{a-a})$, showing the irrefutable role of the surface electrons in the adatom 1D arrangement. In the case of the nearest-neighbor distance probability, the theoretical most probable value for r_{a-a} is 23.3 Å, whereas the experiment showed 25.4 Å. This small difference can be due to the fact that the system is not completely equilibrated, corresponding to a thermal expansion of the spatial distribution. All in all, the agreement between theory and experiment is very satisfactory, confirming that the atomic 1D self-alignment is driven by electronic substrate mediated interactions.

IV. CONCLUSION

Our study presents a bottom-up approach for the organization of one-dimensional Co and Fe strings by using the inherent self-assembly capability of methionine biomolecular nanotemplates on a noble-metal substrate. The dynamics and equilibrium statistics of this 1D self-alignment process have been determined, confirming that the confined surface-state electrons are mediating the underlying long-range indirect interactions. This demonstrates how the spatial arrangement of single atoms can be controlled by a self-assembled nanostructured template steering anisotropic electronic interactions. It is suggested that this methodology can be generally employed for nanoscale control of matter and the positioning of single atomic or molecular species in surface-supported supramolecular architectures. Thus it complements the spectrum of the previously followed atomic manipulation protocols[1–4] and opens avenues to realize ensembles of nanosystems with tailored physical properties such as low-dimensional superstructures of magnetic adatoms[18,40–42] or surface Kondo systems with tunable surface-state occupation.[43–45]

ACKNOWLEDGMENTS

This work was supported by Canada Foundation of Innovation, National Science and Engineering Research Council of Canada, and British Columbia Knowledge Development Fund. A.W.-B., J.R., and W.A. thank the German Academic Exchange Service, the German Research Foundation, and the Swiss National Science Foundation for support, respectively. The theoretical modeling was supported via the German Research Foundation under Programs No. SPP 1165 and No. SPP 1153.

*aeschiff@chem.ubc.ca
†jvb@ph.tum.de

[1] M. F. Crommie, C. P. Lutz, and D. M. Eigler, Science **262**, 218 (1993).
[2] H. Manoharan, C. P. Lutz, and D. M. Eigler, Nature (London) **403**, 512 (2000).
[3] N. Nilius, T. Wallis, and W. Ho, Science **297**, 1853 (2002).
[4] S. Fölsch, P. Hyldgaard, R. Koch, and K. H. Ploog, Phys. Rev. Lett. **92**, 056803 (2004).
[5] P. Gambardella, A. Dallmeyer, K. Malti, M. Malagoli, W. Eberhardt, K. Kern, and C. Carbone, Nature (London) **416**, 301 (2002).
[6] T. Yokoyama, S. Yokoyama, T. Kamikado, Y. Okuno, and S. Mashiko, Nature (London) **413**, 619 (2001).
[7] J. A. Theobald, N. S. Oxtoby, M. A. Phillips, N. R. Champness, and P. H. Beton, Nature (London) **424**, 1029 (2003).
[8] J. V. Barth, J. Weckesser, C. Z. Cai, P. Günter, L. Bürgi, O. Jeandupeux, and K. Kern, Angew. Chem., Int. Ed. **39**, 1230 (2000).
[9] A. Schiffrin, A. Riemann, W. Auwärter, Y. Pennec, A. Weber-Bargioni, D. Cvetko, A. Cossaro, M. Alberto, and J. V. Barth, Proc. Natl. Acad. Sci. U.S.A. **104**, 5279 (2007).
[10] J. V. Barth, G. Costantini, and K. Kern, Nature (London) **437**, 671 (2005).

[11] J. V. Barth, Annu. Rev. Phys. Chem. **58**, 375 (2007).
[12] A. Dmitriev, H. Spillmann, N. Lin, J. V. Barth, and K. Kern, Angew. Chem., Int. Ed. **42**, 2670 (2003).
[13] U. Schlickum *et al.*, Nano Lett. **7**, 3813 (2007).
[14] S. Stepanow, M. Lingenfelder, A. Dmitriev, H. Spillmann, E. Delvigne, N. Lin, X. B. Deng, C. Z. Cai, J. V. Barth, and K. Kern, Nat. Mater. **3**, 229 (2004).
[15] H. F. Ding, V. S. Stepanyuk, P. A. Ignatiev, N. N. Negulyaev, L. Niebergall, M. Wasniowska, C. L. Gao, P. Bruno, and J. Kirschner, Phys. Rev. B **76**, 033409 (2007).
[16] N. Knorr, H. Brune, M. Epple, A. Hirstein, M. A. Schneider, and K. Kern, Phys. Rev. B **65**, 115420 (2002).
[17] J. Repp, F. Moresco, G. Meyer, K. H. Rieder, P. Hyldgaard, and M. Persson, Phys. Rev. Lett. **85**, 2981 (2000).
[18] F. Silly, M. Pivetta, M. Ternes, F. Patthey, J. P. Pelz, and W. D. Schneider, Phys. Rev. Lett. **92**, 016101 (2004).
[19] F. Silly, M. Pivetta, M. Ternes, F. Patthey, J. P. Pelz, and W. D. Schneider, New J. Phys. **6**, 16 (2004).
[20] G. Hörmandinger, Phys. Rev. B **49**, 13897 (1994).
[21] G. Hörmandinger and J. B. Pendry, Phys. Rev. B **50**, 18607 (1994).
[22] N. N. Negulyaev, V. S. Stepanyuk, L. Niebergall, W. Hergert, H. Fangohr, and P. Bruno, Phys. Rev. B **74**, 035421 (2006).
[23] N. N. Negulyaev, V. S. Stepanyuk, W. Hergert, H. Fangohr, and P. Bruno, Surf. Sci. **600**, L58 (2006).
[24] V. S. Stepanyuk, N. N. Negulyaev, L. Niebergall, R. C. Longo, and P. Bruno, Phys. Rev. Lett. **97**, 186403 (2006).
[25] M. L. Merrick, W. Luo, and K. A. Fichthorn, Prog. Surf. Sci. **72**, 117 (2003).
[26] L. Bürgi, O. Jeandupeux, A. Hirstein, H. Brune, and K. Kern, Phys. Rev. Lett. **81**, 5370 (1998).
[27] Y. Pennec, W. Auwärter, A. Schiffrin, A. Weber-Bargioni, A. Riemann, and J. V. Barth, Nat. Nanotechnol. **2**, 99 (2007).
[28] K. Morgenstern, K. F. Braun, and K. H. Rieder, Phys. Rev. Lett. **89**, 226801 (2002).
[29] V. S. Stepanyuk, A. N. Baranov, D. V. Tsivlin, W. Hergert, P. Bruno, N. Knorr, M. A. Schneider, and K. Kern, Phys. Rev. B **68**, 205410 (2003).
[30] W. Auwärter, A. Schiffrin, A. Weber-Bargioni, Y. Pennec, A. Riemann, and J. V. Barth, Int. J. Nanotechnol. **5**, 1171 (2008).
[31] G. Meyer, Rev. Sci. Instrum. **67**, 2960 (1996).
[32] I. Horcas, R. Fernandez, J. M. Gomez-Rodriguez, J. Colchero, J. Gomez-Herrero, and A. M. Baro, Rev. Sci. Instrum. **78**, 013705 (2007).
[33] J. V. Barth, J. Weckesser, G. Trimarchi, M. Vladimirova, A. De Vita, C. Z. Cai, H. Brune, P. Günter, and K. Kern, J. Am. Chem. Soc. **124**, 7991 (2002).
[34] A. Bogicevic, S. Ovesson, P. Hyldgaard, B. I. Lundqvist, H. Brune, and D. R. Jennison, Phys. Rev. Lett. **85**, 1910 (2000).
[35] See EPAPS Document No. E-PRBMDO-78-060827 for STM movie of Co adatoms diffusing at 18 K on Ag(111) in between methionine trenches with widths of 25–35 Å (I_t=0.06 nA, U_{bias}=−400 mV, 750×750 Å^2, and 31 frames for a real time of 10 929 s). For more information on EPAPS, see http://www.aip.org/pubservs/epaps.html.
[36] J. V. Barth, Surf. Sci. Rep. **40**, 75 (2000).
[37] N. Knorr, Ph.D. thesis, EPF Lausanne, 2002.
[38] G. Jahnz, Diploma thesis, University of Hamburg, 2007.
[39] J. V. Barth, T. Zambelli, J. Wintterlin, R. Schuster, and G. Ertl, Phys. Rev. B **55**, 12902 (1997).
[40] V. S. Stepanyuk, L. Niebergall, R. C. Longo, W. Hergert, and P. Bruno, Phys. Rev. B **70**, 075414 (2004).
[41] V. S. Stepanyuk, L. Niebergall, W. Hergert, and P. Bruno, Phys. Rev. Lett. **94**, 187201 (2005).
[42] B. Lazarovits, L. Szunyogh, and P. Weinberger, Phys. Rev. B **73**, 045430 (2006).
[43] J. Merino and O. Gunnarsson, Phys. Rev. Lett. **93**, 156601 (2004).
[44] J. Henzl and K. Morgenstern, Phys. Rev. Lett. **98**, 266601 (2007).
[45] E. Rossi and D. K. Morr, Phys. Rev. Lett. **97**, 236602 (2006).